Size effects in microstructured superconductors and quantum materials

Fermin, R.

1

INTRODUCTION

At the time of writing, the amount of transistors in the processor of the latest smartphones is in the order of 10^{10}. This results from the information processing industry striving to push the boundaries of how small a transistor can be fabricated. Since the 1970s, the average size of a transistor actually halved every two years, an empirical observation that is known as Moore's law. Since we have entered the realm of the ultrasmall, understanding the laws of physics that govern these length scales will prove vital for developing any future computing technologies. Specifically, ones based on novel physics — like superconducting spintronics or neuromorphic computing using correlated electron matter — require a thorough understanding of physical processes at the microscale.

In the case of superconducting spintronics, for example, the field that strives to combine computations using electron spin with the non-dissipative nature of superconductors, the physical processes are magnetism and, naturally, superconductivity. The length scales determining the physics in the latter are the coherence length and London penetration depth. Both are typically between 1 nm and 1 µm (at low temperatures). When reducing the size of superconducting devices to these scales, we need to rethink the relations that normally govern superconductivity on the macro scale. A similar argument can be made for ferromagnets: here, the competition between exchange energy (trying to align the spins) and demagnetization energy (trying to reduce stray fields) causes a ferromagnet to form magnetic domains spontaneously. Reducing the sample size to below the domain size can result in single domain ferromagnets. More importantly, by carefully tuning the geometry of the ferromagnet, a rich variety of magnetic textures, like ferromagnetic vortices and skyrmions, can be stabilized[1–4].

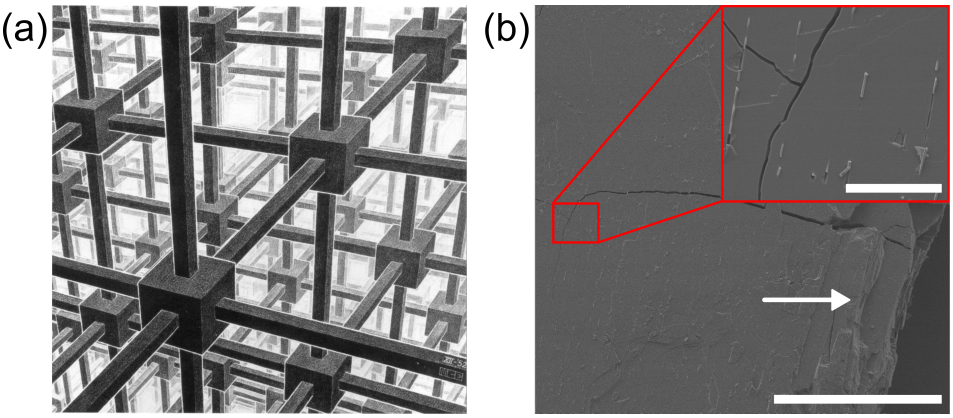

Figure 1.1: (a) *Kubische Ruimteverdeling* by M.C. Escher, how we picture crystalline solids. (b) scanning electron micrograph of an actual macroscopic crystal of Ca_2RuO_4. A large crack is located in the middle of the crystal. Terraced step edges are visible on the side, indicated by the white arrow. The inset shows a scanning electron micrograph of higher magnification. Here some impurities and a zoom of the crack in the crystal can be seen. The scale bar in the main image corresponds to 300 µm; the one in the inset is ten times smaller, namely 30 µm.

Besides probing the laws of physics on the microscale, reducing the size of the studied material improves the controllability of experiments. This is specifically important in the study of correlated electron matter as it involves crystalline form of matter: a periodically ordered lattice of atoms. We picture these materials in their pristine ordered form, namely a repetition of the same unit cell *ad infinitum*, similar to the lithograph *Kubische Ruimteverdeling* by M.C. Escher (see Figure 1.1a). In reality, even the most pure crystals contain micro-cracks, step edges, inclusions of other atoms, and impurities at the macroscopic size level. An example is shown in the scanning electron micrograph of Figure 1.1b. However, when we reduce the system size to mesoscopic levels by cutting out a clean part of the parent compound, we are able to 'zoom in' on a pristine part of the crystal, which significantly improves the controllability of the study.

Typically, microscopic devices are constructed *bottom-up*, meaning their constituents are smaller than the total. For example, by combining lithography and thin film deposition, different material layers are incorporated into a device. This process can be compared to strokes of paint on a canvas. The method faces several difficulties, including the challenging deposition of correlated oxides. In contrast, central to the experiments presented here is a *top-down* technique: by employing a combination of mechanical exfoliation and focused ion beam (FIB) processing, we reduce the size of macroscopic correlated oxide crystals into microstructures. This can be regarded as carving a statue from a larger block of marble. We gain complete control over the size and geometry of the samples while circumventing the need for thin film growth of oxide systems. FIB processing also unlocks the possibility of structuring planar Josephson junctions from macroscopic thin films, with various electrode geometries and feature sizes well below the micrometer scale. For conventional electron beam lithography methods, in con-

trast, any feature size below 1 μm becomes exponentially difficult.

1.1. OUTLINE OF THIS THESIS

This thesis will study the effects of size reduction and geometry on planar Josephson junctions and highly correlated electron matter using transport experiments. The work is divided into three parts, the first of which introduces the basic concepts of superconductivity and Josephson junctions, which are two superconducting electrodes separated by a non-superconducting weak link. Specifically, we present how these concepts are altered upon reducing the size into microscopic geometries by providing a theoretical framework that relates measurable quantities to the superconducting electrode geometry. Besides, we describe a method to fabricate planar Josephson junctions with a normal metal weak link and arbitrary electrode geometry employed to test this theory. In the second part, we replace the normal metal weak link with a ferromagnet to study the interplay between superconductivity and ferromagnetic spin textures. By carefully tuning the geometry of the sample, we show that spin texture can induce superconducting correlations in a single ferromagnet. Furthermore, we find that the bistability of such textures can be utilized to create a non-volatile superconducting memory element. In the final part of this thesis, we examine the isostructural correlated electron oxides Ca_2RuO_4 and Sr_2RuO_4. For the first, we use the crystal size as the principal tool to investigate its Mott-insulating transition: we find the current density required to drive the crystal out of its insulating phase to have a strong size dependence, which has considerable implications for its possible technological implementation. For Sr_2RuO_4, we use microscopic geometries to isolate a single superconducting domain wall, which acts as a Josephson junction. We show that we can control the periodicity of its current-phase relation by applying in-plane fields. Below I will provide more details on each part of this thesis.

1.1.1. PART ONE: JOSEPHSON PHYSICS IN THIN FILM PLANAR JUNCTIONS

The first part will develop a background on superconductivity and Josephson physics. In Chapter 2, I will discuss that superconductivity is a macroscopic manifestation of quantum mechanics. In a regular conducting solid, the electrons are weakly interacting and repel each other due to their negative charge. Besides, electrons are spin-$\frac{1}{2}$ particles and therefore follow Fermi-Dirac statistics. However, this radically changes upon entering the superconducting phase. Below the superconducting transition, a finite positive pair-wise interaction exists between the electrons, letting them form Bosonic composite particles. Based on the change from Fermionic to Bosonic nature of the charge carriers, I derive the basic properties of superconductors in Chapter 2. Besides, Chapter 2 discusses one of the most fundamental superconducting objects: Josephson junctions. These are non-superconducting connections sandwiched between two su-

perconducting electrodes. I will highlight how the quantum nature of superconductors truly shines in these junctions by deriving how the maximum supercurrent (called critical current, I_c) is dependent on an externally applied magnetic field (B), among other basic properties.

In Chapter 3, I will discuss how the properties of a Josephson junction alter when the thickness of the electrodes is reduced below the London penetration depth, forming so-called thin film planar junctions. Specifically, for junctions featuring laterally constrained and arbitrarily shaped electrodes, $I_c(B)$ becomes governed by non-local electrodynamics[5–8]. This expresses itself in $I_c(B)$ becoming completely dependent on the geometry of the electrodes. By extending the theory to ellipsoid and rhomboid geometries, Chapter 3 builds on the work of John Clem, who derived $I_c(B)$ for junctions with a rectangular geometry[9]. Besides, we verify the theory by fabricating elliptically shaped Josephson junctions with various aspect ratios. Finally, we use these results to adjust the Fourier relation between $I_c(B)$ and the critical current distribution in the junction. This is the perfect tool to study the appearance of current channels in the magnetic Josephson junctions, which is the topic of the next part.

1.1.2. PART TWO: MESOSCOPIC SF-HYBRID JOSEPHSON JUNCTIONS

In the second part of this thesis, we study the interplay between magnetic textures and supercurrents. Superconductivity and magnetism are generally antagonistic: in most superconductors, the electrons pair up with opposite spins, whereas the exchange interaction tries to align them. However, over the last 20 years it has been shown that magnetic non-collinearity at the interface of a superconductor can induce long-range triplet superconductivity: pairs of equal spin that can penetrate a ferromagnet over far longer length scales[10–14]. In this part, we combine micromagnetic simulations with the large control over the geometry gained by our top-down fabrication approach to study triplet superconductivity induced directly by spin texture. Specifically, Chapter 4 shows that superconducting triplet correlations can be generated by the vortex magnetization of a single disk-shaped ferromagnet without relying on the conventional combination between spin mixing and spin rotation. Using the analysis developed in the third Chapter, we find the supercurrent to flow in highly localized channels on the rims of the device (aptly named *rim currents*), which are a direct result of an effective spin-orbit coupling caused by the vortex magnetization.

In the fifth Chapter, we examine a more applied example of superconductor-ferromagnet hybrids. Here we show that a transition from circular to elliptical devices can induce bistable magnetic textures at zero applied magnetic field: either the ellipse is magnetized along its long axis, or two vortices are stable near its focal points. Furthermore, the difference in spin-texture is accompanied by a change in critical current, allowing for the creation of a superconducting memory element, which combines the

non-volatility of the ferromagnet with the easy dissipationless read-out of the superconductor. By carefully analyzing the simulations, we are able to explain the change in critical current in terms of the stray fields originating from the different magnetic configurations.

1.1.3. PART THREE: STRONGLY CORRELATED RUTHENIUM OXIDE MICROSTRUCTURES

In Part 3, we will shift gears and leave the topic of thin film Josephson junctions. Instead, we will examine a family of strongly correlated electron systems, namely the *Ruthenates*, which exhibits a rich diversity of phenomena that include Mott insulators[15, 16], unconventional superconductivity[17, 18], and magnetism[19, 20]. The topic of Chapter 6 is the paramagnetic Mott insulator Ca_2RuO_4. This perovskite oxide seems a good candidate for Mott-based electronic devices since it features a metal-to-insulator transition triggered by small current densities[21, 22]. However, whether electronic or thermal effects cause this transition is still under debate since the transition can also be induced by heating the crystal to 357K[23]. In Chapter 6, we use the crystal size itself as the principal tool to investigate the insulator to metal transition. We find a four orders of magnitude increase of the current density required to drive Ca_2RuO_4 out of the insulating phase when reducing the size of the crystals to the micrometer range, shattering the promise of applications at the sub-micrometer level. Besides, we investigate the influence of temperature using microscopic contact thermometry and thermal simulations. We conclude that the size dependence cannot be attributed to Joule heating.

In Chapter 7, we return to the realm of superconductivity by treating the isostructural counterpart of Ca_2RuO_4, where the Ca atoms are substituted by strontium. Ever since the discovery of superconductivity in Sr_2RuO_4 in 1994, its pairing symmetry has posed a challenging conundrum[24]. Already in 1995, it was proposed that superconductivity in Sr_2RuO_4 might be a solid-state analog of the A phase of superfluid ^{3}He: a native triplet superconductor that is degenerate in two chiral ground states[25, 26]. Although this idea has been contested since 2019[27, 28], and the current proposals widely vary, the community agrees that the pairing symmetry is of two-component nature[29, 30]. Such a two-component order parameter is likely expected to host multi-domain superconductivity. In a previous work, we utilized microstructures to trap a single superconducting domain wall[31]. This manifested itself as the formation of spontaneous Josephson junctions in the nominally clean crystal. In Chapter 7, we extend this work by measuring the Shapiro response of these junctions. Not only does this serve as a definite proof of the existence of these spontaneous junctions, it additionally allows for characterizing the periodicity of their current-phase relation. We find that, under the application of in-plane (i.e., ab-plane) magnetic fields, the periodicity of the current-phase relation can halve, as evidenced by the appearance of half-integer Shapiro steps.

1

Furthermore, we show that in-plane fields can decrease the pinning of the domains, resulting in a bistability of the critical current. This allows for switching between a high critical current state and a low critical current state by applying a large enough positive or negative bias current. We finish by reinterpreting these results based on the latest literature regarding the pairing symmetry in Sr_2RuO_4.

REFERENCES

[1] Prejbeanu, I. L. *et al.* In-plane reversal mechanisms in circular Co dots. *J. Appl. Phys.* **91**, 7343–7345 (2002).

[2] Natali, M. *et al.* Correlated magnetic vortex chains in mesoscopic cobalt dot arrays. *Phys. Rev. Lett.* **88**, 157203 (2002).

[3] Chui, C. P., Ma, F. & Zhou, Y. Geometrical and physical conditions for skyrmion stability in a nanowire. *AIP Adv.* **5**, 047141 (2015).

[4] Winkler, T. B. *et al.* Skyrmion states in disk geometry. *Phys. Rev. Applied* **16**, 044014 (2021).

[5] Pearl, J. Current distribution in superconducting films carrying quantized fluxoids. *Appl. Phys. Lett.* **5**, 65–66 (1964).

[6] Ivanchenko, Y. & Soboleva, T. Nonlocal interaction in Josephson junctions. *Phys. Lett. A* **147**, 65–69 (1990).

[7] Abdumalikov, A. A., Jr., Alfimov, G. L. & Malishevskii, A. S. Nonlocal electrodynamics of Josephson vortices in superconducting circuits. *Supercond. Sci. Technol.* **22**, 023001 (2009).

[8] Boris, A. A. *et al.* Evidence for nonlocal electrodynamics in planar Josephson junctions. *Phys. Rev. Lett.* **111**, 117002 (2013).

[9] Clem, J. R. Josephson junctions in thin and narrow rectangular superconducting strips. *Phys. Rev. B* **81**, 144515 (2010).

[10] Bergeret, F. S., Volkov, A. F. & Efetov, K. B. Long-range proximity effects in superconductor-ferromagnet structures. *Phys. Rev. Lett.* **86**, 4096 (2001).

[11] Bergeret, F. S., Volkov, A. F. & Efetov, K. B. Odd triplet superconductivity and related phenomena in superconductor-ferromagnet structures. *Rev. Mod. Phys.* **77**, 1321 (2005).

[12] Houzet, M. & Buzdin, A. I. Long range triplet Josephson effect through a ferromagnetic trilayer. *Phys. Rev. B* **76**, 060504 (2007).

[13] Khaire, T. S., Khasawneh, M. A., Pratt, W. P. & Birge, N. O. Observation of spin-triplet superconductivity in Co-based Josephson junctions. *Phys. Rev. Lett.* **104**, 137002 (2010).

[14] Robinson, J. W. A., Witt, J. D. S. & Blamire, M. G. Controlled injection of spin-triplet supercurrents into a strong ferromagnet. *Science* **329**, 59 (2010).

[15] Nakatsuji, S., Ikeda, S.-i. & Maeno, Y. Ca_2RuO_4: new Mott insulators of layered ruthenate. *J. Phys. Soc. Jpn.* **66**, 1868–1871 (1997).

[16] Zhu, M. *et al.* Colossal magnetoresistance in a Mott insulator via magnetic field-driven insulator-metal transition. *Phys. Rev. Lett.* **116**, 216401 (2016).

[17] Maeno, Y., Kittaka, S., Nomura, T., Yonezawa, S. & Ishida, K. Evaluation of spin-triplet superconductivity in Sr_2RuO_4. *J. Phys. Soc. Jpn.* **81**, 011009 (2012).

[18] Leggett, A. J. & Liu, Y. Symmetry properties of superconducting order parameter in Sr_2RuO_4: A brief review. *J. Supercond. Nov. Magn.* **34**, 1647—-1673 (2020).

[19] Cao, G., McCall, S., Crow, J. E. & Guertin, R. P. Observation of a metallic antiferromagnetic phase and metal to nonmetal transition in $Ca_3Ru_2O_7$. *Phys. Rev. Lett.* **78**, 1751–1754 (1997).

[20] Grigera, S. A. *et al.* Magnetic field-tuned quantum criticality in the metallic ruthenate $Sr_3Ru_2O_7$. *Science* **294**, 329–332 (2001).

[21] Nakamura, F. *et al.* Electric-field-induced metal maintained by current of the Mott insulator Ca_2RuO_4. *Sci. Rep.* **3**, 2536 (2013).

[22] Okazaki, R. *et al.* Current-induced gap suppression in the mott insulator Ca_2RuO_4. *J. Phys. Soc. Jpn.* **82**, 103702 (2013).

[23] Alexander, C. S. *et al.* Destruction of the Mott insulating ground state of Ca_2RuO_4 by a structural transition. *Phys. Rev. B* **60**, R8422(R) (1999).

[24] Maeno, Y. *et al.* Superconductivity in a layered perovskite without copper. *Nature* **372**, 532–534 (1994).

[25] Rice, T. M. & Sigrist, M. Sr_2RuO_4: an electronic analogue of ^{3}He? *J. Phys.: Condens. Matter* **7**, L648 (1995).

[26] Rice, M. An analogue of superfluid ^{3}He. *Nature* **396**, 627–628 (1998).

[27] Pustogow, A. *et al.* Constraints on the superconducting order parameter in Sr_2RuO_4 from oxygen-17 nuclear magnetic resonance. *Nature* **574**, 72–75 (2019).

[28] Petsch, A. N. *et al.* Reduction of the spin susceptibility in the superconducting state of Sr_2RuO_4 observed by polarized neutron scattering. *Phys. Rev. Lett.* **125**, 217004 (2020).

[29] Ghosh, S. *et al.* Thermodynamic evidence for a two-component superconducting order parameter in Sr_2RuO_4. *Nat. Phys.* **17**, 199–204 (2021).

[30] Benhabib, S. *et al.* Ultrasound evidence for a two-component superconducting order parameter in Sr_2RuO_4. *Nat. Phys.* **17**, 194–198 (2021).

[31] Yasui, Y. *et al.* Spontaneous emergence of Josephson junctions in homogeneous rings of single-crystal Sr_2RuO_4. *npj Quantum Mater.* **5**, 21 (2020).